Materials **2014**, *7*, 7548-7565; doi:10.3390/ma7117548

OPEN ACCESS

materials

ISSN 1996-1944

www.mdpi.com/journal/materials

Article

1,7-Bis-(*N*,*N*-dialkylamino)perylene Bisimides: Facile Synthesis and Characterization as Near-Infrared Fluorescent Dyes

Kew-Yu Chen * and Che-Wei Chang

Department of Chemical Engineering, Feng Chia University, Taichung 40724, Taiwan;
E-Mail: m0111617@fcu.edu.tw

* Author to whom correspondence should be addressed; E-Mail: kyuchen@fcu.edu.tw;
Tel.: +886-4-2451-7250 (ext. 3683); Fax: +886-4-2451-0890.

External Editor: Dirk Poelman

Received: 20 October 2014; in revised form: 10 November 2014 / Accepted: 13 November 2014 / Published: 24 November 2014

Abstract: Three symmetric alkylamino-substituted perylene bisimides with different *n*-alkyl chain lengths (*n* = 6, 12, or 18), 1,7-bis-(*N*,*N*-dialkylamino)perylene bisimides (**1a**–**1c**), were synthesized under mild condition and were characterized by ^{1}H NMR, ^{13}C NMR and high resolution mass spectroscopy. Their optical and electrochemical properties were measured using UV-Vis and emission spectroscopic techniques as well as cyclic voltammetry (CV). These compounds show deep green color in both solution and solid state, and are highly soluble in dichloromethane and even in nonpolar solvents such as hexane. The shapes of the absorption spectra of **1a**–**1c** in the solution and solid state were found to be almost the same, indicating that the long alkyl chains could efficiently prevent intermolecular contact and aggregation. They show a unique charge transfer emission in the near-infrared region, of which the peak wavelengths exhibit strong solvatochromism. The dipole moments of the molecules have been estimated using the Lippert–Mataga equation, and upon excitation, they show larger dipole moment changes than that of 1,7-diaminoperylene bisimide (**2**). Moreover, all the dyes exhibit two irreversible one-electron oxidations and two quasi-reversible one-electron reductions in dichloromethane at modest potentials. Complementary density functional theory calculations performed on these chromophores are reported in order to rationalize their electronic structure and optical properties.

Keywords: near-infrared fluorescent dyes; 1,7-bis-(*N*,*N*-dialkylamino)perylene bisimides; intramolecular charge transfer; solvatochromism; Lippert–Mataga equation; density functional theory calculations

1. Introduction

Derivatives of perylene bisimide (PBI) have continuously attracted significant attention due to their applications in molecular electronic devices, such as light-emitting diodes [1–5], LCD color filters [6,7], organic field-effect transistors (OFETs) [8–13], light-harvesting arrays [14,15], photovoltaic cells [16–25], molecular wires [26,27], and photochromic materials [28,29]. PBIs have also been utilized as building blocks to construct supramolecular or artificial photosynthetic systems [30–33]. These organic molecules are advantageous due to their high molar absorptivities, high photochemical and optical stabilities, reversible redox properties, ease of synthetic modification and excellent thermal stability [34–55]. The electronic characteristics of PBIs can also be fine-tuned by introducing different substituents at the bay-positions (1,6,7,12-positions) of the conjugated perylene core. Based on these rules, a number of perylene bisimide derivatives with either electron-withdrawing or electron-donating groups have been reported in the literature, including: (a) perfluoroalkyl-substituted PBIs [56,57]; (b) cyano-substituted PBIs [58,59], (c) nitro-substituted PBIs [60–62]; (d) ferrocenyl-substituted PBIs [63,64], (e) aryl-substituted PBIs [65,66], (f) boryl-substituted PBIs [67]; (g) alkyl-substituted PBIs [68]; (h) piperidinyl-substituted PBIs [69–71], (i) pyrrolidinyl-substituted PBIs [72–74]; (j) amino-substituted PBIs [75,76], (k) alkylamino-substituted PBIs [77–79], (l) alkoxy-substituted PBIs [80–84]; (m) hydroxy-substituted PBIs [85,86], *etc.*

To date, a promising strategy for introducing substituents onto the PBI core is bromination or chlorination of perylene dianhydride. Subsequently, replacement of these halogens is readily executed by traditional substitution reactions or by metal-catalyzed cross-coupling reactions. However, both of these methods are usually accompanied by extensive debromination [77] and stringent reaction conditions such as high temperatures, and absence of oxygen and water. In an effort to expand the scope of PBI-based chromophores available for designing systems for colorful dyes and self-assembly, we synthesized a series of blue dyes based on 1,7-diaminoperylene bisimides [76]. We herein report on the introduction of different long alkyl chains of 1,7-diaminoperylene bisimide (**2**) affording chromophores (**1a**–**1c**) that are deep green in color and that readily undergo two irreversible one-electron oxidations and two quasi-reversible one-electron reductions.

2. Experimental Section

2.1. General

The starting materials such as perylene-3,4,9,10-tetracarboxyldianhydride, acetic acid, cyclohexylamine, cerium (IV) ammonium nitrate (CAN), tin (II) chloride dihydrate ($SnCl_2.2H_2O$), *N*-methyl-2-pyrrolidinone (NMP), tetrahydrofuran (THF), sodium hydride (NaH), 1-iodohexane ($C_6H_{13}I$), 1-iodododecane ($C_{12}H_{25}I$), and 1-iodooctadecane ($C_{18}H_{37}I$) were purchased from Merck

(Whitehouse Station, NJ, USA), ACROS (Pittsburgh, PA, USA) and Sigma–Aldrich (St. Louis, MO, USA). Solvents were distilled freshly according to standard procedure. Column chromatography was performed using silica gel Merck Kieselgel *si* 60 (40–63 mesh). ^{1}H and ^{13}C NMR spectra were recorded in $CDCl_3$ on a Bruker 400 MHz NMR spectrometer (Palo Alto, CA, USA). Mass spectra were recorded on a VG70-250S mass spectrometer (Tokyo, Japan). The absorption and emission spectra were measured using a Jasco V-570 UV–Vis spectrophotometer (Tokyo, Japan) and a Hitachi F-7000 fluorescence spectrophotometer (Tokyo, Japan), respectively. Cyclic voltammetry (CV) was performed with a CH instruments (Austin, TX, USA) at a potential rate of 200 mV/s in a 0.1 M solution of tetrabutylammonium hexafluorophosphate ($TBAPF_6$) in dichloromethane. Platinum and $Ag/AgNO_3$ electrodes were used as counter and reference electrodes, respectively.

2.2. Synthesis

2.2.1. Perylene Bisimide (**4**)

A suspension of perylene dianhydride (900 mg, 2.3 mmol), cyclohexylamine (570 mg, 5.8 mmol), and acetic acid (500 mg, 8.3 mmol) in 50 mL of *N*-methyl-2-pyrrolidinone was stirred at 80 °C under nitrogen for 8 h. After the mixture was cooled to room temperature, the precipitate was isolated by filtration, washed with 200 mL of MeOH, and dried in a vacuum. The crude product was purified by silica gel column chromatography with eluent CH_2Cl_2 to afford **4** (950 mg, 75%). Characterization data: **4**: ^{1}H NMR (400 MHz, $CDCl_3$) δ 8.64 (d, J = 8.0 Hz, 4H), 8.60 (d, J = 8.0 Hz, 4H), 5.05 (m, 2H), 2.58 (m, 4H), 1.91 (m, 4H), 1.76 (m, 6H), 1.36–1.46 (m, 6H). MS (FAB): m/z (relative intensity) 555 (M^+, 100); HRMS calcd. for $C_{36}H_{31}N_2O_4$ 555.2284, found 555.2290.

2.2.2. Synthesis of 1,7-Dinitroperylene Bisimide (**3**)

A mixture of perylene bisimide **4** (900 mg, 1.6 mmol), cerium (IV) ammonium nitrate (CAN) (2.4 g, 4.4 mmol), nitric acid (0.1 M, 6.0 mL) and dichloromethane (150 mL) was stirred at 25 °C under N_2 for 48 h. The mixture was neutralized with 10% KOH and extracted with CH_2Cl_2. After solvent was removed, the crude product was purified by silica gel column chromatography with eluent CH_2Cl_2 to afford **3** (837 mg, 80%). Characterization data: **3**: ^{1}H NMR (400 MHz, $CDCl_3$) δ 8.78 (s, 2H), 8.67 (d, J = 8.0 Hz, 2H), 8.28 (d, J = 8.0 Hz, 2H), 4.99 (m, 2H), 2.51 (m, 4H), 1.92 (m, 4H), 1.74 (m, 6H), 1.46 (m, 4H), 1.36 (m, 2H); MS (FAB): m/z (relative intensity) 645 ($M+H^+$, 100); HRMS calcd. for $C_{36}H_{29}O_8N_4$ 645.1985, found 645.1981.

2.2.3. Synthesis of 1,7-Diaminoperylene Bisimide (**2**)

Tin chloride dihydrate (1.5 g, 7.2 mmol) and **3** (0.8 g, 1.2 mmol) were suspended in 60 mL of THF, and stirred 20 min. The solvent was refluxed with stirring for 6 h at 80 °C. THF was removed at the rotary evaporator, and the residue was dissolved in ethyl acetate and washed with 10% NaOH solution and brine. The organic layer was dried over anhydrous $MgSO_4$ and the filtrate was concentrated under reduced pressure. The crude product was purified by silica gel column chromatography with eluent ethyl acetate/n-hexane (2/3) to afford **2** (595 mg, 85%). Characterization data: **2**: ^{1}H NMR (400 MHz, $CDCl_3$) δ 8.87 (d, J = 8.4 Hz, 2H), 8.43 (d, J = 8.4 Hz, 2H), 8.14 (s, 2H), 5.04, (m, 2H), 4.94 (s, 4H),

2.61 (m, 4H), 1.93 (m, 4H), 1.74 (m, 6H), 1.36–1.54 (m, 6H); MS (FAB): m/z (relative intensity) 585 ($M+H^+$, 100); HRMS calcd. for $C_{36}H_{33}O_4N_4$ 585.2502, found 585.2504.

2.2.4. General Procedure for Alkylation (**1a**–**1c**)

A mixture of solution of **2** (410 mg, 0.70 mmol), sodium hydride (97%, 200 mg, 8.00 mmol) and dry THF (60 mL) was stirred at 0 °C under N_2 for 30 min. Alkyl iodide (4.20 mmol) was then added and the resulting mixture was stirred for 8 h. The resulting mixture was diluted with 15 mL of water and extracted with CH_2Cl_2. The crude product was purified by silica gel column chromatography with eluent ethyl acetate/n-hexane (1/2) to afford **1a** (**1b** or **1c**) in 75% yield. Characterization data: **1a**: ^{1}H NMR (400 MHz, $CDCl_3$) δ 9.21 (d, *J* = 8.0 Hz, 2H), 8.45 (s, 2H), 8.38 (d, *J* = 8.0 Hz, 2H), 5.03 (m, 2H), 3.45 (m, 4H), 3.15 (m, 4H), 2.57 (m, 4H), 1.87 (m, 4H), 1.15–1.75 (m, 44H), 0.82 (t, *J* = 6.4 Hz, 12H); ^{13}C NMR (100 MHz, $CDCl_3$) δ 164.51, 164.21, 148.51, 135.42, 130.32, 128.21, 125.31, 124.29, 122.90, 122.74, 122.63, 121.10, 53.77, 52.54, 31.42, 29.17, 27.46, 26.89, 26.60, 25.52, 22.49, 13.90; MS (FAB): m/z (relative intensity) 921 ($M+H^+$, 100); HRMS calcd. for $C_{60}H_{81}O_4N_4$ 921.6256, found 921.6250. Selected data for **1b**: ^{1}H NMR (400 MHz, $CDCl_3$)δ 9.20 (d, *J* = 8.4 Hz, 2H), 8.45 (s, 2H), 8.37 (d, *J* = 8.4 Hz, 2H), 5.04 (m, 2H), 3.46 (m, 4H), 3.17 (m, 4H), 2.60 (m, 4H), 1.87 (m, 4H), 1.12–1.75 (m, 92H), 0.85 (t, *J* = 6.5 Hz, 12H); ^{13}C NMR (100 MHz, $CDCl_3$) δ 164.40, 164.06, 148.46, 135.32, 130.25, 128.13, 125.25, 124.23, 122.81, 122.70, 122.59, 121.05, 53.71, 52.43, 31.81, 29.53, 29.45, 29.24, 29.21, 29.12, 27.46, 27.16, 26.55, 25.47, 22.59, 14.01; MS (FAB): m/z (relative intensity) 1258 ($M+H^+$, 100); HRMS calcd. for $C_{84}H_{129}O_4N_4$ 1258.0014, found 1258.0004. Selected data for **1c**: ^{1}H NMR (400 MHz, $CDCl_3$)δ 9.19 (d, *J* = 8.4 Hz, 2H), 8.45 (s, 2H), 8.38 (d, *J* = 8.4 Hz, 2H), 5.04 (m, 2H), 3.45 (m, 4H), 3.15 (m, 4H), 2.60 (m, 4H), 1.87 (m, 4H), 1.14–1.74 (m, 140H), 0.86 (t, *J* = 6.4 Hz, 12H); ^{13}C NMR (100 MHz, $CDCl_3$) δ 164.45, 164.12, 148.51, 135.39, 130.32, 128.20, 125.30, 124.30, 122.89, 122.76, 122.66, 121.12, 53.77, 52.51, 31.91, 29.68, 29.52, 29.34, 29.27, 29.19, 27.53, 27.23, 26.60, 25.53, 22.66, 14.07; MS (FAB): m/z (relative intensity) 1595 ($M+H^+$, 100); HRMS calcd. for $C_{108}H_{177}O_4N_4$ 1595.3803, found 1595.3815.

3. Results and Discussion

3.1. Synthesis

Scheme 1 depicts the chemical structures and synthetic routes of symmetric 1,7-dialkylamino substituted PBIs (**1a**–**1c**). Synthesis starts from an imidization [87] of perylene dianhydride (**5**) by reaction with cyclohexylamine ($C_6H_{11}NH_2$). The dinitration can then be achieved by a reaction of perylene bisimide (**4**) with cerium (IV) ammonium nitrate (CAN) and HNO_3 under ambient temperature for 48 h [60], giving 1,6- and 1,7-dinitroperylene bisimides in high yields of *ca.* 80%. The regioisomeric 1,6- and 1,7-dinitroperylene bisimides can be successfully separated by high performance liquid chromatography (HPLC). Pure 1,7-regioisomer (**3**) can also be obtained through repetitive crystallizations. The reduction of 1,7-dinitroperylene bisimide (**3**) by tin (II) chloride dihydrate ($SnCl_2.2H_2O$) in refluxing THF obtained 1,7-diaminoperylene bisimide (**2**). Finally, three 1,7-dialkylamino substituted perylene bisimide derivatives (**1a**–**1c**) with different *n*-alkyl chain lengths (*n* = 6, 12, or 18) can be synthesized by the alkylation of **2** with the corresponding alkyl

halides. These compounds show deep green color in both solution and solid state, and are highly soluble in dichloromethane (Figure 1) and even in nonpolar solvents such as hexane. The symmetric structure of 1,7-bis-(*N*,*N*-dialkylamino)perylene bisimides (**1a**–**1c**) can be verified by the presence of three signals (one singlet and two doublet signals) at δ 8.3–9.3 ppm in the ^{1}H NMR spectrum, which indicates that there are only three different kinds of protons in the conjugated perylene core (Figure 2). Detailed synthetic procedures and product characterization are provided in the Experimental Section and Supplementary Materials (Figures S1–S6).

Scheme 1. The synthetic route for **1a**–**1c**.

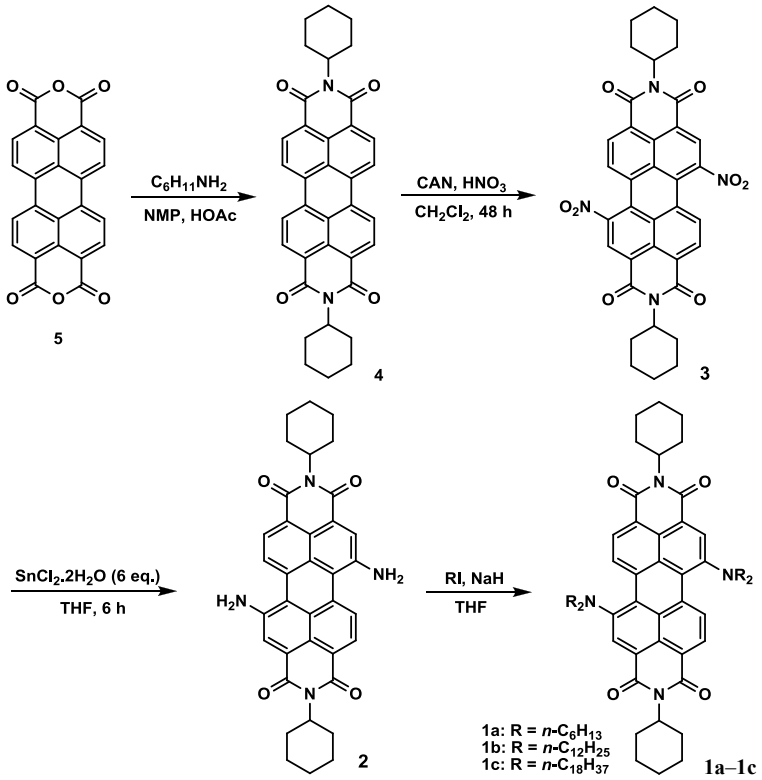

Figure 1. Solubility of **1a**–**1c** in dichloromethane (25 °C).

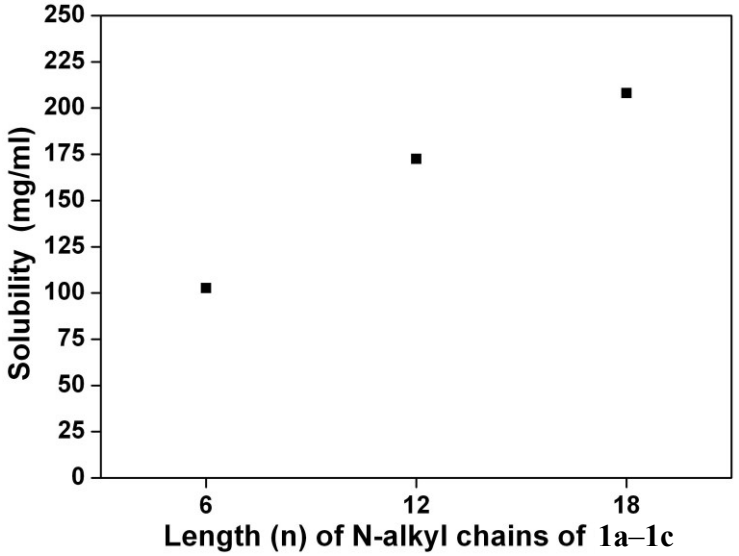

Figure 2. ^{1}H NMR (400 MHz, $CDCl_3$) spectra of **1a**.

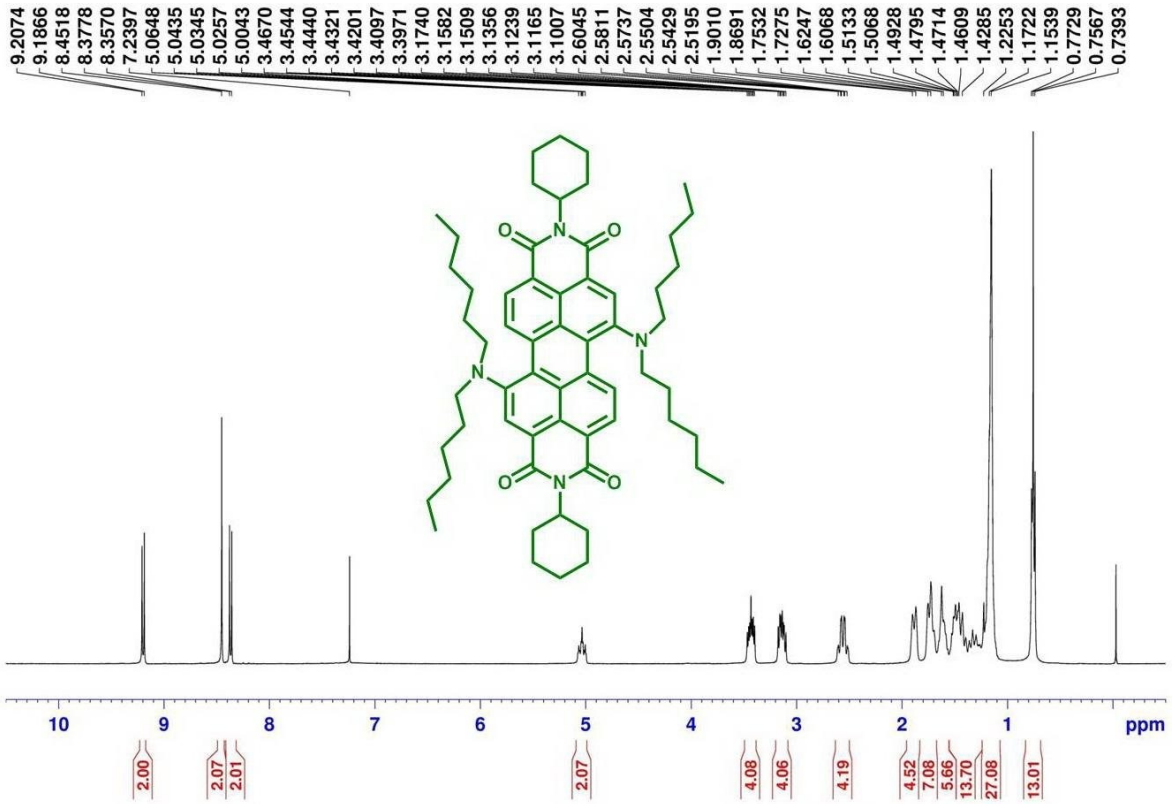

3.2. Optical Properties

Figure 3 shows the steady state absorption spectra of the green dye **1a**, the blue dye **2**, and the red dye **3** in dichloromethane. The spectra of **1b** and **1c** can be found in the Supplementary Materials (Figures S7 and S8). The absorption spectrum of 1,7-dinitroperylene bisimide (**3**) is nearly identical with the spectrum of the non-substituted perylene bisimide (**4**), but they do not show fluorescence [60]. On the other hand, the reduction of **3** to **2** switches the substituents from electron-withdrawing nitro groups to electron-donating amino groups and causes a distinct red shift. The spectra of 1,7-diamino substituted (**2**) and 1,7-dialkylamino substituted (**1a**–**1c**) PBIs are dominated by very broad absorption bands that cover a large part of the visible spectrum (350–800 nm). These broad bands are typical for perylene bisimide derivatives *N*-substituted at the bay-core positions, due to charge transfer absorption [77]. The longest wavelength absorption band of 1,7-diaminoperylene bisimide (**2**: 620 nm) is red-shifted relative to that of 1,7-dinitroperylene bisimide (**3**: 515 nm), but it is blue-shifted relative to that of 1,7-dialkylaminoperylene bisimide (**1a**: 698 nm). It appears that the inductive effect of the alkyl groups in **1a**–**1c** causes an additional red shift. Additionally, the longest wavelength absorption band of **1a**–**1c** exhibits a red shift when the solvent polarity increases (Table 1), which is consistent with previous studies [75].

Figure 3. Normalized absorption spectra of **1a**, **2**, and **3** in dichloromethane solution.

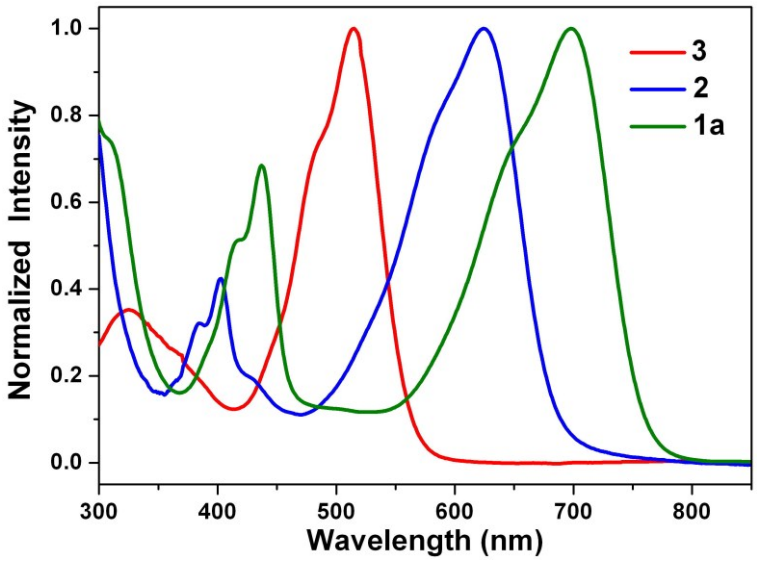

Table 1. Summary of optical absorption and emission properties of **1a**–**1c** in various solvents.

1a/1b/1c	λ_{abs} (nm) [a]	λ_{em} (nm) [a]	Stokes shift (nm)	Φ [b] × 10^2
cyclohexane	667/670/670	711/714/716	44/44/48	3.03/4.74/3.14
diethyl ether	675/676/676	726/725/726	51/46/51	0.44/0.80/0.92
ethyl acetate	687/688/687	741/740/740	57/54/55	0.22/0.41/0.42
dichloromethane	698/702/701	755/758/758	52/55/54	0.20/0.40/0.41
acetonitrile	699/703/703	760/760/761	61/56/57	0.25/0.26/0.26

[a] Measured at 2×10^{-5} M; [b] Determined with *N*,*N*'-dioctyl-3,4,9,10-perylenedicarboximide as reference [31].

Figure 4 depicts the steady state emission spectra of **1a** in solvents of varying polarity, where those of **1b** and **1c** can be found in the Supplementary Materials (Figures S9 and S10). Unlike the small shift in absorption spectra, the fluorescence spectra of **1a**–**1c** are largely red-shifted if there is any increase of the solvent polarity, which indicates strong intramolecular charge transfer characteristics for the excited states of **1a**–**1c** (Table 1). Using the well-established fluorescence solvatochromic shift method [88], we measured the stabilization of the excited-states of **1a**–**1c** and compared these results to those of **2**. The change of magnitudes for dipole moments between ground and excited states, *i.e.*, $\Delta\mu = \left|\vec{\mu}_e - \vec{\mu}_g\right|$, can be calculated by the Lippert–Mataga equation and expressed as:

$$\bar{\nu}_a - \bar{\nu}_f = \frac{2}{hc}\left(\vec{\mu}_e - \vec{\mu}_g\right)^2 a_0^{-3} + const. \quad (1)$$

where h is the Planck constant, c is the speed of light, and a_0 denotes the cavity radius in which the solute resides, $\bar{\nu}_a - \bar{\nu}_f$ is the Stokes shift of the absorption and emission peak maximum, and Δf is the orientation polarizability defined as:

$$\Delta f = f(\varepsilon) - f(n^2) = \frac{\varepsilon - 1}{2\varepsilon + 1} - \frac{n^2 - 1}{2n^2 + 1} \quad (2)$$

Figure 4. Normalized emission spectra of **1a** in various solvents.

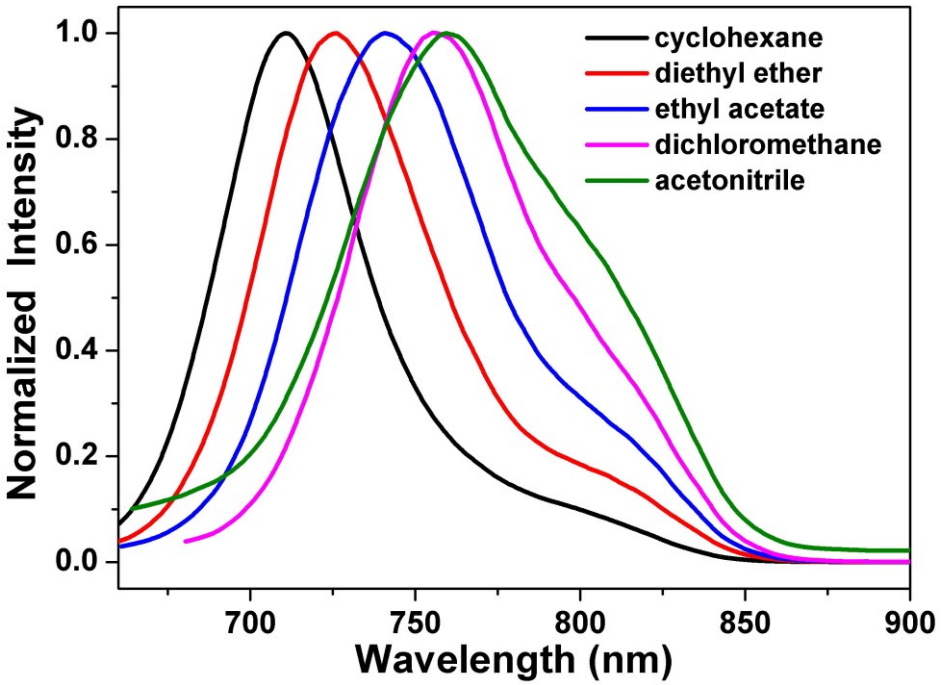

The plot of the Stokes shift $\bar{\upsilon}_a - \bar{\upsilon}_f$ as a function of Δf is sufficiently linear for **1a**–**1c** (Figure 5). Accordingly, $\Delta\mu = \left|\vec{\mu}_e - \vec{\mu}_g\right|$ values can be estimated as 7.9 D, 9.1 D and 9.7 D for **1a**–**1c**. These values indicate that the 1,7-dialkyamino-substituted PBIs (**1a**–**1c**) have larger dipole moment changes than that (7.4 D) of the 1,7-diamino-substituted compound (**2**).

Figure 5. Lippert–Mataga plots for **1a** (blue line), **1b** (green line), and **1c** (red line). The solvents from left to right are (1) cyclohexane; (2) diethyl ether; (3) ethyl acetate; (4) dichloromethane, (5) acetonitrile.

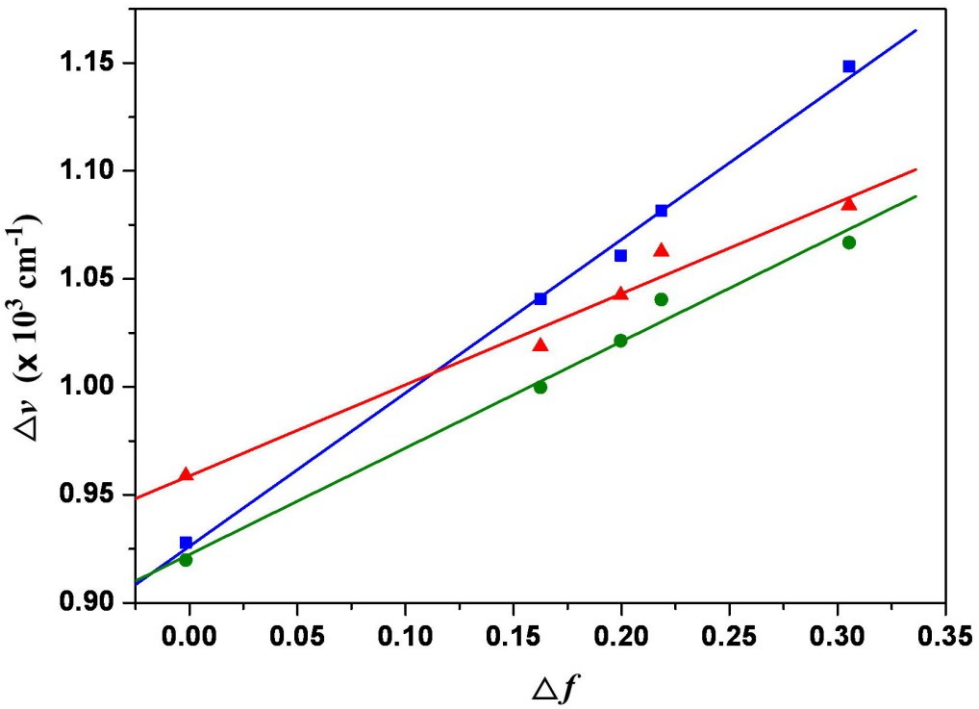

3.3. Quantum Chemistry Computation

To gain better insight into the molecular structures and electronic properties of **1a**–**1c**, quantum chemical calculations were performed using density functional theory (DFT) at the B3LYP/6-31G** level. Figure 6 shows the highest occupied molecular orbitals (HOMOs) and the lowest unoccupied molecular orbitals (LUMOs) of **1a** and **2**. The HOMO of all amino-substituted PBIs (**1a**–**1c** and **2**) is delocalized chiefly on the amino group and the perylene core, while the LUMO is extended from the central perylene core to the bisimide groups. Table 2 summarizes the calculated and experimental parameters for perylene bisimide derivatives **1a**–**1c**. Obviously, the HOMO/LUMO energy levels of **1a**–**1c** and **2** are higher than those of **3** and **4**, which can be explained by the fact that the amino substituent is a strong electron-donating group and hence increases both the HOMO and LUMO energy levels. Furthermore, the calculated HOMO–LUMO band gap energies of **1a**–**1c** are in good agreement with the experimental data (Table 2).

Figure 6. Calculated frontier orbitals for **1a** and **2**. The upper structures show the lowest unoccupied molecular (LUMOs) and the lower ones show the highest occupied molecular orbitals (HOMOs). Methyl groups replace the hexyl groups for clarity.

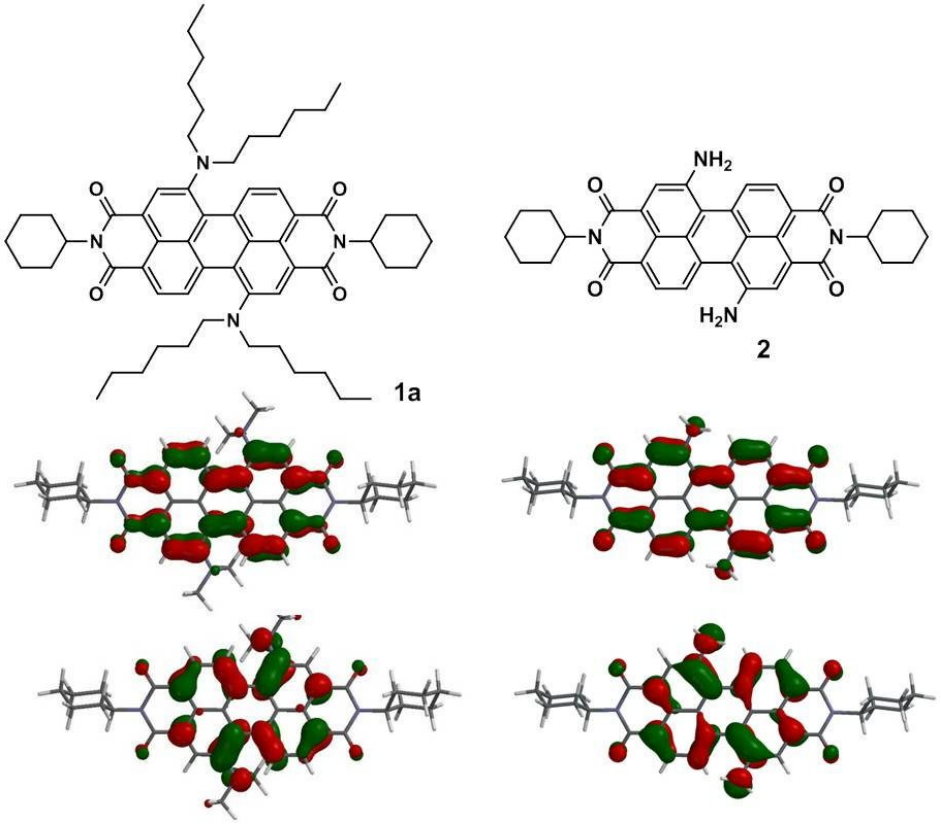

DFT calculations also demonstrate that the ground-state geometries of the perylene core have different core twist angles (Figure 7 and Table 2), *i.e.*, approximate dihedral angles between the two naphthalene subunits attached to the central benzene ring; these are ~17.53° and ~17.54° for **1a**, ~17.55° and ~17.57° for **1b**, ~17.58° and ~17.59° for **1c**, ~19.21° and ~19.43° for **2**, and ~17.02° and ~17.12° for **3**, and all are larger than those of **4** (~0.00°). As a whole, the core twist angles of the diamino-substituted PBIs (**1** and **2**) are slightly larger than that of the dinitro-substituted compound (**3**).

Figure 7. DFT (B3LYP/6-31G**) geometry-optimized structures of **1a** (left) and **2** (right) shown with view along the long axis. For computational purposes, methyl groups replace the cyclohexyl groups at the imide positions.

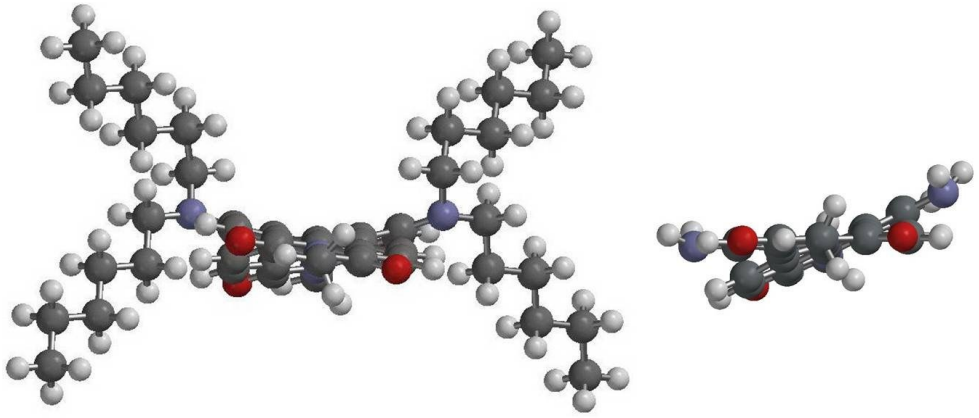

Table 2. Calculated and experimental parameters for perylene bisimide derivatives.

Compound	HOMO [a]	LUMO [a]	E_g [a]	E_g [b]	μ_g [c]	μ_e [d]	Twisting angle (°)
1a	−5.24	−3.12	2.12	1.76	2.9	10.8	17.53, 17.54
1b	−5.24	−3.12	2.12	1.76	3.0	12.1	17.55, 17.57
1c	−5.23	−3.11	2.12	1.77	3.0	12.7	17.58, 17.59
2	−5.33	−3.05	2.28	2.14	2.6	7.8	19.21, 19.43
3	−6.57	−4.11	2.46	2.40	–	–	17.02, 17.12
4	−5.94	−3.46	2.48	2.38	–	–	0.00, 0.00

[a] Calculated by DFT/B3LYP (in eV); [b] At absorption maxima (E_g = 1240/λ_{max}, in eV); [c] Ground-state dipole moment (calculated by DFT/B3LYP, in Debye); [d] Excited-state dipole moment (in Debye).

3.4. Electrochemical Properties

Figure 8 shows the cyclic voltammograms of **1a**–**1c**. These dyes undergo two irreversible one-electron oxidations and two quasi-reversible one-electron reductions in dichloromethane at modest potentials. Table 3 summarizes the redox potentials and the HOMO and LUMO energy levels estimated from cyclic voltammetry (CV) for **1a**–**1c**. It is apparent that both the first oxidation and the first reduction potentials are shifted toward more negative (positive) values with introducing strongly electron-donating (electron-withdrawing) groups onto the perylene core, while both the HOMO and LUMO energy levels increase (decrease) with the trend. The HOMO/LUMO energy levels of **1a**, **1b**, **1c**, and **2** are estimated to be −5.25/−3.49, −5.23/−3.47, −5.22/−3.45, and −5.39/−3.25 eV, respectively. The HOMO–LUMO energy gaps of **1a**–**1c** are found to be almost the same, which indicates that different *N*-alkyl chain lengths do not significantly affect the band gap energies.

Figure 8. The cyclic voltammograms of **1a** (blue line), **1b** (green line), and **1c** (red line) measured in dichloromethane solution with ferrocenium/ferrocene as an internal standard, at 200 mV/s.

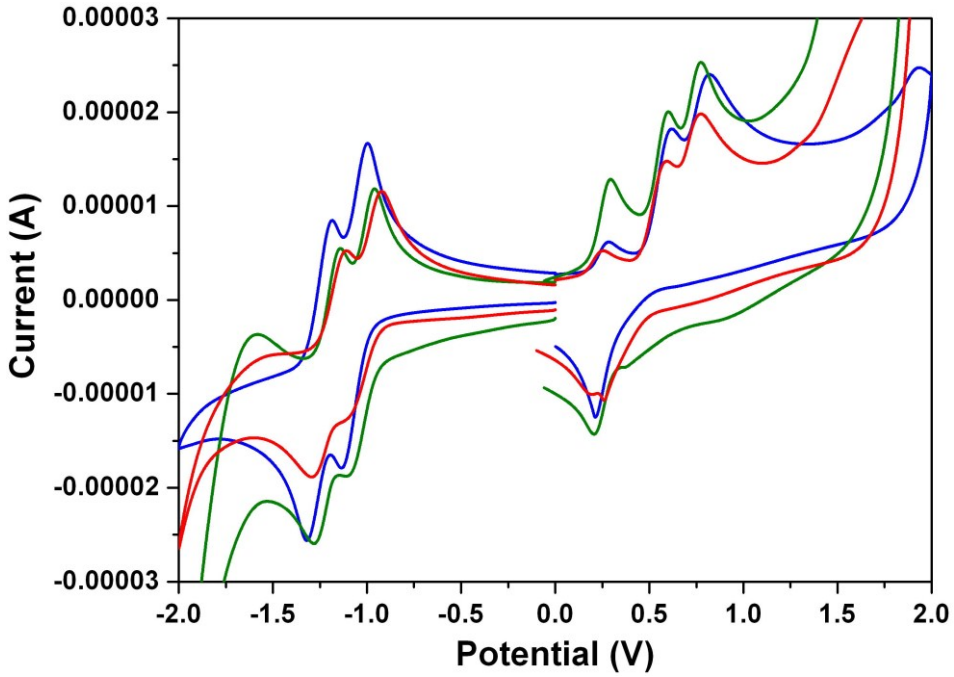

Table 3. Summary of half-wave redox potentials, HOMO and LUMO energy levels for perylene bisimide derivatives.

Compound	$E^{+}_{1/2}$ [a]	$E^{2+}_{1/2}$ [a]	$E^{-}_{1/2}$ [a]	$E^{2-}_{1/2}$ [a]	HOMO [b]	LUMO [b]
1a	0.62	0.82	−1.06	−1.22	−5.25	−3.49
1b	0.60	0.77	−1.04	−1.20	−5.23	−3.47
1c	0.59	0.77	−1.02	−1.19	−5.22	−3.45
2	0.79	1.17	−1.15	−1.24	−5.39	−3.25
3 [c]	–	–	−0.09	−0.34	−6.75	−4.35
4 [c]	–	–	−0.46	−0.76	−6.36	−3.98

[a] Measured in a solution of 0.1 M tetrabutylammonium hexafluorophosphate ($TBAPF_6$) in dichloromethane *versus* SCE (in V); [b] Calculated from $E_{HOMO} = -4.88 - (E_{oxd} - E_{Fc/Fc+})$, $E_{LUMO} = E_{HOMO} + E_g$; [c] Estimated *versus* vacuum level from $E_{LUMO} = -4.44 - E_{(1)}$.

3.5. Stacking Behaviors of Dyes in Solution and Solid State

Figure 9 depicts the absorption spectra recorded for thin drop-cast films of **1a**–**1c**. The shapes of the absorption spectra of **1a**–**1c** in solid state and in solution are found to be almost the same in view of wavelength range (absorption of up to 800 nm for **1a**–**1c**) and peak positions, which indicates that it is difficult for **1a**–**1c** to form π-aggregates. Thus, we can ascertain that the long alkyl chains not only largely increases the solubility of **1a**–**1c** compared with **2**, but also efficiently reduces intermolecular contact and aggregation.

Figure 9. Normalized absorption spectra of **1a**–**1c** in neat film.

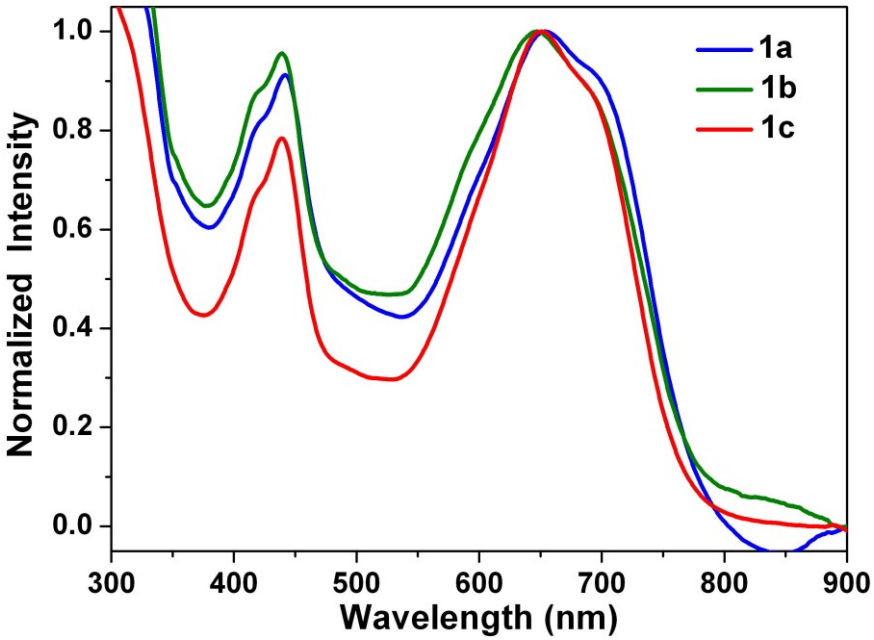

4. Conclusions

We have successfully synthesized three green dyes based on 1,7-dialkylamino substituted PBIs (**1a**–**1c**). All the new PBI dyes are highly soluble in dichloromethane and even in nonpolar solvents such as hexane. The shapes of the absorption spectra of **1a**–**1c** in solution and solid state are found to be virtually the same, which indicates that the long alkyl chains can efficiently prevent intermolecular contact and aggregation. They exhibit a unique charge transfer emission in the near-infrared region, of which the peak wavelengths exhibit strong solvatochromism. Upon excitation, they show larger dipole moment changes than that of **2**; the dipole moments of these compounds have been estimated using DFT calculations and the Lippert–Mataga equation. In addition, they undergo two irreversible one-electron oxidations and two quasi-reversible one-electron reductions in dichloromethane at modest potentials. Research on their applications to near-infrared fluorescence imaging [89–91] is currently in progress.

Supplementary Materials

Supplementary materials can be accessed at: http://www.mdpi.com/1996-1944/7/11/7548/s1.

Acknowledgments

The project was supported by the Ministry of Science and Technology (MOST 103-2113-M-035-001) in Taiwan. The authors appreciate the Precision Instrument Support Center of Feng Chia University for providing the fabrication and measurement facilities.

Author Contributions

Kew-Yu Chen supervised the project. Che-Wei Chang measured the data.

Conflicts of Interest

The authors declare no conflict of interest.

References

1. Ventura, B.; Langhals, H.; Böck, B.; Flamigni, L. Phosphorescent perylene imides. *Chem. Commun.* **2012**, *48*, 4226–4228.
2. Matsui, M.; Wang, M.; Funabiki, K.; Hayakawa, Y.; Kitaguchi, T. Properties of novel perylene-3,4:9,10-tetracarboxidiimide-centred dendrimers and their application as emitters in organic electroluminescence devices. *Dyes Pigm.* **2007**, *74*, 169–175.
3. Damaceanu, M.-D.; Constantin, C.-P.; Bruma, N.; Pinteala, M. Tuning of the color of the emitted light from new polyperyleneimides containing oxadiazole and siloxane moieties. *Dyes Pigm*. **2013**, *99*, 228–239.
4. Lucenti, E.; Botta, C.; Cariati, E.; Righetto, S.; Scarpellini, M.; Tordin, E.; Ugo, R. New organic-inorganic hybrid materials based on perylene diimide–polyhedral oligomeric silsesquioxane dyes with reduced quenching of the emission in the solid state. *Dyes Pigm*. **2013**, *96*, 748–755.
5. Pan, J.; Zhu, W.; Li, S.; Zeng, W.; Cao, Y.; Tian, H. Dendron-functionalized perylene diimides with carrier-transporting ability for red luminescent materials. *Polymer* **2005**, *46*, 7658–7669.
6. Choi, J.; Lee, W.; Sakong, C.; Yuk, S.B.; Park, J.S.; Kim, J.P. Facile synthesis and characterization of novel coronene chromophores and their application to LCD color filters. *Dyes Pigm.* **2012**, *94*, 34–39.
7. Sakong, C.; Kim, Y.D.; Choi, J.H.; Yoon, C.; Kim, J.P. The synthesis of thermally-stable red dyes for LCD color filters and analysis of their aggregation and spectral properties. *Dyes Pigm.* **2011**, *88*, 166–173.
8. Jones, B.A.; Ahrens, M.J.; Yoon, M.H.; Facchetti, A.; Marks, T.J.; Wasielewski, M.R. High-mobility air-stable *n*-type semiconductors with processing versatility: Dicyanoperylene-3,4:9,10-bis(dicarboximides). *Angew. Chem. Int. Ed.* **2004**, *43*, 6363–6366.
9. Kim, F.S.; Guo, X.; Watson, M.D.; Jenekhe, S.A. High-mobility ambipolar transistors and high-gain inverters from a donor-acceptor copolymer semiconductor. *Adv. Mater.* **2009**, *21*, 1–5.
10. Würthner, F.; Stolte, M. Naphthalene and perylene diimides for organic transistors. *Chem. Commun.* **2011**, *47*, 5109–5115.
11. Reghu, R.R.; Bisoyi, H.K.; Grazulevicius, J.V.; Anjukandi, P.; Gaidelis, V.; Jankauskas, V. Air stable electron-transporting and ambipolar bay substituted perylene bisimides. *J. Mater. Chem.* **2011**, *21*, 7811–7819.
12. Zaumseil, J.; Sirringhaus, H. Electron and ambipolar transport in organic field-effect transistors. *Chem. Rev.* **2007**, *107*, 1296–1323.
13. Locklin, J.; Li, D.; Mannsfeld, S.C.B.; Borkent, E.J.; Meng, H.; Advincula, R.; Bao, Z. Organic thin film transistors based on cyclohexyl-substituted organic semiconductors. *Chem. Mater.* **2005**, *17*, 3366–3374.

14. Li, X.; Sinks, L.E.; Rybtchinski, B.; Wasielewski, M.R. Ultrafast aggregate-to-aggregate energy transfer within self-assembled light-harvesting columns of zinc phthalocyanine tetrakis (perylenediimide). *J. Am. Chem. Soc.* **2004**, *126*, 10810–10811.
15. Rybtchinski, B.; Sinks, L.E.; Wasielewski, M.R. Combining light-harvesting and charge separation in a self-assembled artificial photosynthetic system based on perylenediimide chromophores. *J. Am. Chem. Soc.* **2004**, *126*, 12268–12269.
16. Kozma, E.; Kotowski, D.; Catellani, M.; Luzzati, S.; Famulari, A.; Bertini, F. Synthesis and characterization of new electron acceptor perylene diimide molecules for photovoltaic applications. *Dyes Pigm.* **2013**, *99*, 329–338.
17. Li, J.; Dierschke, F.; Wu, J.; Grimsdale, A.C.; Müllen, K. Poly(2,7-carbazole) and perylene tetracarboxydiimide: A promising donor/acceptor pair for polymer solar cells. *J. Mater. Chem.* **2006**, *16*, 96–100.
18. Dinçalp, H.; Aşkar, Z.; Zafer, C.; İçli, S. Effect of side chain substituents on the electron injection abilities of unsymmetrical perylene diimide dyes. *Dyes Pigm.* **2011**, *91*, 182–191.
19. Ramanan, C.; Semigh, A.L.; Anthony, J.E.; Marks, T.J.; Wasielewski, M.R. Competition between singlet fission and charge separation in solution-processed blend films of 6,13-bis(triisopropylsilylethynyl)-pentacene with sterically-encumbered perylene-3,4:9,10-bis(dicarboximide)s. *J. Am. Chem. Soc.* **2012**, *134*, 386–397.
20. Shibano, Y.; Umeyama, T.; Matano, Y.; Imahori, H. Electron-donating perylene tetracarboxylic acids for dye-sensitized solar cells. *Org. Lett.* **2007**, *9*, 1971–1974.
21. Kozma, E.; Catellani, M. Perylene diimides based materials for organic solar cells. *Dyes Pigm.* **2013**, *98*, 160–179.
22. Tian, H.; Liu, P.H.; Zhu, W.; Gao, E.; Wu, D.J.; Cai, S. Synthesis of novel multi-chromophoric soluble perylene derivatives and their photosensitizing properties with wide spectral response for SnO_2 nanoporous electrode. *J. Mater. Chem.* **2000**, *10*, 2708–2715.
23. Choi, H.; Paek, S.; Song, J.; Kim, C.; Cho, N.; Ko, J. Synthesis of annulated thiophene perylene bisimide analogues: Their applications to bulk heterojunction organic solar cells. *Chem. Commun.* **2011**, *47*, 5509–5511.
24. Huang, C.; Barlow, S.; Marder, S.R. Perylene-3,4,9,10-tetracarboxylic acid diimides: Synthesis, physical properties, and use in organic electronics. *J. Org. Chem.* **2011**, *76*, 2386–2407.
25. Wang, H.Y.; Peng, B.; Wei, W. Solar cells based on perylene bisimide derivatives. *Prog. Chem.* **2008**, *20*, 1751–1760.
26. Weiss, E.A.; Ahrens, M.J.; Sinks, L.E.; Gusev, A.V.; Ratner, M.A.; Wasielewski, M.R. Making a molecular wire: Charge and spin transport through para-phenylene oligomers. *J. Am. Chem. Soc.* **2004**, *126*, 5577–5584.
27. Wilson, T.M.; Tauber, M.J.; Wasielewski, M.R. Toward an *n*-type molecular wire: Electron hopping within linearly linked perylenediimide oligomers. *J. Am. Chem. Soc.* **2009**, *131*, 8952–8957.
28. Berberich, M.; Krause, A.M.; Orlandi, M.; Scandola, F.; Würthner, F. Toward fluorescent memories with nondestructive readout: Photoswitching of fluorescence by intramolecular electron transfer in a diaryl ethene-perylene bisimide photochromic system. *Angew. Chem. Int. Ed.* **2008**, *47*, 6616–6619.

29. Tan, W.; Li, X.; Zhang, J.; Tian, H. A photochromic diarylethene dyad based on perylene diimide. *Dyes Pigm.* **2011**, *89*, 260–265.
30. Lu, X.; Guo, Z.; Sun, C.; Tian, H.; Zhu, W. Helical Assembly induced by hydrogen bonding from chiral carboxylic acids based on perylene bisimides. *J. Phys. Chem. B* **2011**, *115*, 10871–10876.
31. Würthner, F. Perylene bisimide dyes as versatile building blocks for functional supramolecular architectures. *Chem. Commun.* **2004**, *14*, 1564–1579.
32. Wasielewski, M.R. Self-assembly strategies for integrating light harvesting and charge separation in artificial photosynthetic systems. *Acc. Chem. Res.* **2009**, *42*, 1910–1921.
33. Kaur, B.; Bhattacharya, S.N.; Henry, D.J. Interpreting the near-infrared reflectance of a series of perylene pigments. *Dyes Pigm.* **2013**, *99*, 502–511.
34. Georgiev, N.I.; Sakr, A.R.; Bojinov, V.B. Design and synthesis of novel fluorescence sensing perylene diimides based on photoinduced electron transfer. *Dyes Pigm.* **2011**, *91*, 332–339.
35. Langhals, H.; Kirner, S. Novel fluorescent dyes by the extension of the core of perylenetetracarboxylic bisimides. *Eur. J. Org. Chem.* **2000**, *2*, 365–380.
36. Liang, Y.; Wang, H.; Wang, D.; Liu, H.; Feng, S. The synthesis, morphology and liquid-crystalline property of polysiloxane-modified perylene derivative. *Dyes Pigm.* **2012**, *95*, 260–267.
37. Cazacu, M.; Vlad, A.; Airinei, A.; Nicolescu, A.; Stoica, I. New imides based on perylene and siloxane derivatives. *Dyes Pigm.* **2011**, *90*, 106–113.
38. Kaur, B.; Quazi, N.; Ivanov, I.; Bhattacharya, S.N. Near-infrared reflective properties of perylene derivatives. *Dyes Pigm.* **2012**, *92*, 1108–1113.
39. Boobalan, G.; Imran, P.S.; Nagarajan, S. Synthesis of highly fluorescent and water soluble perylene bisimide. *Chin. Chem. Lett.* **2012**, *23*, 149–153.
40. Cui, Y.; Wu, Y.; Liu, Y.; Yang, G.; Liu, L.; Fu, H.; Li, Z.; Wang, S.; Wang, Z.; Chen, Y. PEGylated nanoparticles of diperylene bisimides with high efficiency of $^1O_2$ generation. *Dyes Pigm*. **2013**, *97*, 129–133.
41. Wang, R.; Shi, Z.; Zhang, C.; Zhang, A.; Chen, J.; Guo, W.; Sun, Z. Facile synthesis and controllable bromination of asymmetrical intermediates of perylene monoanhydride/monoimide diester. *Dyes Pigm*. **2013**, *98*, 450–458.
42. Luo, M.-H.; Chen, K.-Y. Asymmetric perylene bisimide dyes with strong solvatofluorism. *Dyes Pigm.* **2013**, *99*, 456–464.
43. Kang, H.; Jiang, W.; Wang, Z. Construction of well-defined butadiynylene-linked perylene bisimide arrays via cross-coupling. *Dyes Pigm.* **2013**, *97*, 244–249.
44. Shin, I.S.; Hirsch, T.; Ehrl, B.; Jang, D.H.; Wolfbeis, O.S.; Hong, J.I. Efficient fluorescence "turn-on" sensing of dissolved oxygen by electrochemical switching. *Anal. Chem.* **2012**, *84*, 9163–9168.
45. Habuchi, S.; Fujiwara, S.; Yamamoto, T.; Vacha, M.; Tezuka, Y. Single-molecule study on polymer diffusion in a melt state: Effect of chain topology. *Anal. Chem.* **2013**, *85*, 7369–7376.
46. Daimon, T.; Nihei, E. Fabrication of a poly(3-octylthiophene-2,5-diyl) electrochemiluminescence device assisted by perylene. *Materials* **2013**, *6*, 1704–1717.
47. Sharma, G.D.; Kurchania, R.; Ball, R.J.; Roy, M.S.; Mikroyannidis, J.A. Effect of deoxycholic acid on the performance of liquid electrolyte dye-sensitized solar cells using a perylene monoimide derivative. *Int. J. Photoenergy*. **2012**, doi:10.1155/2012/983081.

48. Tsai, H.Y.; Chang, C.W.; Chen, K.Y. 1,6- and 1,7-Regioisomers of asymmetric and symmetric perylene bisimides: synthesis, characterization and optical properties. *Molecules* **2014**, *19*, 327–341.
49. El-Daly, S.A.; Alamry, K.A.; Asiri, A.M.; Hussein, M.A. Spectral characteristics and fluorescence quenching of N,N′-bis(4-pyridyl)-3,4:9,10-perylenebis(dicarboximide) (BPPD). *J. Lumin.* **2012**, *132*, 2747–2752.
50. Tsai, H.Y.; Chen, K.Y. Synthesis and optical properties of novel asymmetric perylene bisimides. *J. Lumin.* **2014**, *149*, 103–111.
51. Yang, T.; Guan, Q.; Guo, X.; Meng, L.; Du, M.; Jiao, K. Direct and freely switchable detection of target genes engineered by reduced graphene oxide-poly(*m*-aminobenzenesulfonic acid) nanocomposite via synchronous pulse electrosynthesis. *Anal. Chem.* **2013**, *85*, 1358–1366.
52. Liao, D.; Chen, J.; Zhou, H.; Wang, Y.; Li, Y.; Yu, C. *In situ* formation of metal coordination polymer: A strategy for fluorescence turn-on assay of acetylcholinesterase activity and inhibitor screening. *Anal. Chem.* **2013**, *85*, 2667–2672.
53. Naveenraj, S.; Raj, M.R. Anandan, S. Binding interaction between serum albumins and perylene-3,4,9,10-tetracarboxylate—A spectroscopic investigation. *Dyes Pigm.* **2012**, *94*, 330–337.
54. Zhang, L.; Wang, Y.; Yu, J.; Zhang, G.; Cai, X.; Wu, Y.; Wang, L. A colorimetric and fluorescent sensor based on PBIs for palladium detection. *Tetrahedron Lett.* **2013**, *54*, 4019–4022.
55. Boobalan, G.; Imran, P.M.; Ramkumar, S.G.; Nagarajan, S. Fabrication of luminescent perylene bisimide nanorods. *J. Lumin.* **2014**, *146*, 387–393.
56. Yuan, Z.; Li, J.; Xiao, Y.; Li, Z.; Qian, X. Core-perfluoroalkylated perylene diimides and naphthalene diimides: Versatile synthesis, solubility, electrochemistry, and optical properties. *J. Org. Chem.* **2010**, *75*, 3007–3016.
57. Li, Y.; Tan, L.; Wang, Z.; Qian, H.; Shi, Y.; Hu, W. Air-stable *n*-type semiconductor: Core-perfluoroalkylated perylene bisimides. *Org. Lett.* **2008**, *10*, 529–532.
58. Weitz, R.T.; Amsharov, K.; Zschieschang, U.; Villas, E.B.; Goswami, D.K.; Burghard, M.; Dosch, H.; Jansen, M.; Kern, K.; Klauk, H. Organic *n*-channel transistors based on core-cyanated perylene carboxylic diimide derivatives. *J. Am. Chem. Soc.* **2008**, *130*, 4637–4645.
59. Jones, B.A.; Facchetti, A.; Wasielewski, M.R.; Marks, T.J. Tuning orbital energetics in arylene diimide semiconductors. Materials design for ambient stability of *n*-type charge transport. *J. Am. Chem. Soc.* **2007**, *129*, 15259–15278.
60. Chen, K.Y.; Chow, T.J. 1,7-Dinitroperylene bisimides: Facile synthesis and characterization as *n*-type organic semiconductors. *Tetrahedron Lett.* **2010**, *51*, 5959–5963.
61. Chen, Z.J.; Wang, L.M.; Zou, G.; Zhang, L.; Zhang, G.J.; Cai, X.F.; Teng, M.S. Colorimetric and ratiometric luorescent chemosensor for fluoride ion based on perylene diimide derivatives. *Dyes Pigm.* **2012**, *94*, 410–415.
62. Kong, X.; Gao, J.; Ma, T.; Wang, M.; Zhang, A.; Shi, Z.; Wei, Y. Facile synthesis and replacement reactions of mono-substituteded perylene bisimide dyes. *Dyes Pigm.* **2012**, *95*, 450–454.
63. Goretzki, G.; Davies, E.S.; Argent, S.P.; Warren, J.E.; Blake, A.J.; Champness, N.R. Building multistate redox-active architectures using metal-complex functionalized perylene bis-imides. *Inorg. Chem.* **2009**, *48*, 10264–10274.

64. Dhokale, B.; Gautam, P.; Misra, R. Donor-acceptor perylenediimide-ferrocene conjugates: Synthesis, photophysical, and electrochemical properties. *Tetrahedron Lett.* **2012**, *53*, 2352–2354.
65. Chao, C.C.; Leung, M.K. Photophysical and electrochemical properties of 1,7-diaryl-substituted perylene diimides. *J. Org. Chem.* **2005**, *70*, 4323–4331.
66. Miasojedovasa, A.; Kazlauskasa, K.; Armonaitea, G.; Sivamuruganb, V.; Valiyaveettilb, S.; Grazuleviciusc, J.V.; Jursenasa, S. Concentration effects on emission of bay-substituted perylene diimide derivatives in a polymer matrix. *Dyes Pigm.* **2012**, *92*, 1285–1291.
67. Dey, S.; Efimov, A.; Lemmetyinen, H. Bay region borylation of perylene bisimides. *Eur. J. Org. Chem.* **2011**, *30*, 5955–5958.
68. Handa, N.V.; Mendoza, K.D.; Shirtcliff, L.D. Syntheses and properties of 1,6 and 1,7 perylene diimides and tetracarboxylic dianhydrides. *Org. Lett.* **2011**, *13*, 4724–4727.
69. Fan, L.; Xu, Y.; Tian, H. 1,6-Disubstituted perylene bisimides: Concise synthesis and characterization as near-infrared fluorescent dyes. *Tetrahedron Lett.* **2005**, *46*, 4443–4447.
70. Rohr, U.; Kohl, C.; Müllen, K.; van de Craats, A.; Warman, J. Liquid crystalline coronene derivatives. *J. Mater. Chem.* **2001**, *11*, 1789–1799.
71. Rajasingh, P.; Cohen, R.; Shirman, E.; Shimon, L.J.W.; Rybtchinski, B. Selective bromination of perylene diimides under mild conditions. *J. Org. Chem.* **2007**, *72*, 5973–5979.
72. Dubey, R.K.; Efimov, A.; Lemmetyinen, H. 1,7- And 1,6-regioisomers of diphenoxy and dipyrrolidinyl substituted perylene diimides: Synthesis, separation, characterization, and comparison of electrochemical and optical properties. *Chem. Mater.* **2011**, *23*, 778–788.
73. Zhao, Y.; Wasielewski, M.R. 3,4:9,10-Perylenebis(dicarboximide) chromophores that function as both electron donors and acceptors. *Tetrahedron Lett.* **1999**, *40*, 7047–7050.
74. Ma, Y.S.; Wang, C.H.; Zhao, Y.J.; Yu, Y.; Han, C.X.; Qiu, X.J.; Shi, Z. Perylene diimide dyes aggregates: Optical properties and packing behavior in solution and solid state. *Supramol. Chem.* **2007**, *19*, 141–149.
75. Chen, K.Y.; Fang, T.C.; Chang, M.J. Synthesis, photophysical and electrochemical properties of 1-aminoperylene bisimides. *Dyes Pigm.* **2011**, *92*, 517–523.
76. Tsai, H.Y.; Chen, K.Y. 1,7-Diaminoperylene bisimides: Synthesis, optical and electrochemical properties. *Dyes Pigm.* **2013**, *96*, 319–327.
77. Ahrens, M.J.; Tauber, M.J.; Wasielewski, M.R. Bis(n-octylamino)perylene-3,4:9,10-bis(dicarboximide)s and their radical cations: Synthesis, electrochemistry, and ENDOR spectroscopy. *J. Org. Chem.* **2006**, *71*, 2107–2114.
78. Alvino, A.; Franceschin, M.; Cefaro, C.; Borioni, S.; Ortaggi, G.; Bianco, A. Synthesis and spectroscopic properties of highly water-soluble perylene derivatives. *Tetrahedron* **2007**, *63*, 7858–7865.
79. Wang, H.; Kaiser, T.E.; Uemura, S.; Würthner, F. Perylene bisimide J-aggregates with absorption maxima in the NIR. *Chem. Commun.* **2008**, *10*, 1181–1183.
80. Dinçalp, H.; Kızılok, Ş.; İçli, S. Fluorescent macromolecular perylene diimides containing pyrene or indole units in bay positions. *Dyes Pigm.* **2010**, *86*, 32–41.
81. Zhao, C.; Zhang, Y.; Li, R.; Li, X.; Jiang, J. Di(alkoxy)- and di(alkylthio)-substituted perylene-3,4;9,10-tetracarboxy diimides with tunable electrochemical and photophysical properties. *J. Org. Chem.* **2007**, *72*, 2402–2410.

82. Ren, H.; Li, J.; Zhang, T.; Wang, R.; Gao, Z.; Liu, D. Synthesis and properties of novel perylenebisimide-cored dendrimers. *Dyes Pigm.* **2011**, *91*, 298–303.
83. Zhang, X.; Pang, S.; Zhang, Z.; Ding, X.; Zhang, S.; He, S.; Zhan, C. Facile synthesis of 1-bromo-7-alkoxyl perylene diimide dyes: Toward unsymmetrical functionalizations at the 1,7-positions. *Tetrahedron Lett.* **2012**, *53*, 1094–1097.
84. Feng, J.; Wang, D.; Wang, S.; Zhang, L.; Li, X. Synthesis and properties of novel perylenetetracarboxylic diimide derivatives fused with BODIPY units. *Dyes Pigm.* **2011**, *89*, 23–28.
85. Fin, A.; Petkova, I.; Doval, D.A.; Sakai, N.; Vauthey, E.; Matile, S. Naphthalene-and perylenediimides with hydroquinones, catechols, boronic esters and imines in the core. *Org. Biomol. Chem.* **2011**, *9*, 8246–8252.
86. Perrin, L.; Hudhomme, P. Synthesis, electrochemical and optical absorption properties of new perylene-3,4:9,10-bis(dicarboximide) and perylene-3,4:9,10-bis(benzimidazole) derivatives. *Eur. J. Org. Chem.* **2011**, *28*, 5427–5440.
87. Luzina, E.L.; Popov, A.V. Synthesis and anticancer activity evaluation of 3,4-mono- and bicyclosubstituted *N*-(het)aryl trifluoromethyl succinimides. *J. Fluor. Chem.* **2014**, *168*, 121–127.
88. Lakowicz, J.R. *Principles of Fluorescence Spectroscopy*; 2nd Ed.; Plenum: New York, NY, USA, 1999.
89. Mawn, T.M.; Popov, A.V.; Delikatny, E.J. A quantitative continuous enzyme assay of intramolecularly quenched fluorogenic phospholipase substrates for molecular imaging. *Anal. Biochem.* **2012**, *422*, 96–102.
90. Mawn, T.M.; Popov, A.V.; Beardsley, N.J.; Stefflova, K.; Milkevitch, M.; Zheng, G.; Delikatny, E.J. *In vivo* detection of phospholipase C by enzyme-activated near-infrared probes. *Bioconjug. Chem.* **2011**, *22*, 2434–2443.
91. Popov, A.V.; Mawn, T.M.; Kim, S.; Zheng, G.; Delikatny, E.J. Design and synthesis of phospholipase C and A_2-activatable near-infrared fluorescent smart probes. *Bioconjug. Chem.* **2010**, *21*, 1724–1727.